ISSN 1063-7834, Physics of the Solid State, 2010, Vol. 52, No. 2, pp. 298–305. © Pleiades Publishing, Ltd., 2010.
Original Russian Text © Yu.L. Raĭkher, V.I. Stepanov, S.V. Stolyar, V.P. Ladygina, D.A. Balaev, L.A. Ishchenko, M. Balasoiu, 2010, published in Fizika Tverdogo Tela, 2010, Vol. 52, No. 2, pp. 277–284.

MAGNETISM
AND FERROELECTRICITY

Magnetic Properties of Biomineral Particles Produced by Bacteria *Klebsiella Oxytoca*

Yu. L. Raĭkher[a, *], V. I. Stepanov[a], S. V. Stolyar[b, c], V. P. Ladygina[d], D. A. Balaev[b, c], L. A. Ishchenko[c], and M. Balasoiu[e]

[a] *Institute of Continuum Media Mechanics, Ural Division, Russian Academy of Sciences, ul. Akademika Koroleva 1, Perm, 614013 Russia*

* *raikher@icmm.ru*

[b] *Kirensky Institute of Physics, Siberian Branch, Russian Academy of Sciences, Akademgorodok 50, Krasnoyarsk, 660036 Russia*

[c] *Siberian Federal University, pr. Svobody 79, Krasnoyarsk, 660041 Russia*

[d] *International Scientific Center for Research of Organism under Extreme Conditions, Krasnoyarsk Scientific Center, Siberian Branch, Russian Academy of Sciences, Akademgorodok, Krasnoyarsk, 660036 Russia*

[e] *Joint Institute for Nuclear Research, ul. Joliot-Curie 6, Dubna, Moscow oblast, 141980 Russia*

Received May 13, 2009

Abstract—Ferrihydrite nanoparticles (2–5 nm in size) produced by bacteria *Klebsiella oxytoca* in the course of biomineralization of iron salt solutions from a natural medium exhibit unique magnetic properties: they are characterized by both the antiferromagnetic order inherent in a bulk ferrihydrite and the spontaneous magnetic moment due to the decompensation of spins in sublattices of a nanoparticle. The magnetic susceptibility enhanced by the superantiferromagnetism effect and the magnetic moment independent of the magnetic field provide the possibility of magnetically controlling these natural objects. This has opened up the possibilities for their use in nanomedicine and bioengineering. The results obtained from measurements of the magnetic properties of the ferrihydrite produced by *Klebsiella oxytoca* in its two main crystalline modifications are reported, and the data obtained are analyzed theoretically. This has made it possible to determine numerical values of the magnetic parameters of real biomineral nanoparticles.

DOI: 10.1134/S1063783410020125

1. BIOMINERALIZED IRON OXIDES: GENERAL OBSERVATIONS

In recent years, a growing interest has been expressed by researchers in disperse systems containing antiferromagnetic nanoparticles. The most known and rather widespread material of this type is ferritin, which is a cytosolic (intracellular) complex in the form of a shell approximately 12 nm in outside diameter that consists of 24 polypeptide units of the protein referred to as the apoferritin (see, for example, [1, 2]). The inner cavity (~8 nm in diameter) of the apoferritin shell is occupied by the iron hydroxide (ferrihydrite) nanoparticle, sometimes, with a small impurity of ferric hydroxide phosphate with the chemical formula $[FeO(OH)_8][FeO(H_2PO_4)]$ up to 7 nm in diameter. The mineral core of the ferritin has a pronounced crystal structure with an antiferromagnetic spin ordering of trivalent iron atoms.

The ferritin exists in the form of natural colloids (ferritins of bacteria, plants, animals, and humans), which play an important role in the metabolism [3–6], and in the form of synthetic nanodispersions (artificial ferritins, binary ferritins) intended for investigations and applications [1, 7, 8]. In this work, we study the ferrihydrite synthesized by bacteria *Klebsiella oxytoca*. These microorganisms are well known in industrial microbiology and geochemistry owing to their ability to mineralize large specific amounts of iron under anaerobic conditions with the accumulation of the ferrihydrite. The ferrihydrite is formed as a result of the oxidation reaction $Fe^{2+} \longrightarrow Fe^{3+}$, which ensures the energy for the vital functions of bacteria. The "fuel" (Fe^{2+} ions) either comes from the environment or is formed from the ferrihydrite accumulated by a cell as a result of its photochemical reduction, i.e., in the light [9].

By all appearances, unlike magnetosensitive bacteria *Magnetospirillum*, the magnetization of biomineral nanoparticles is of little significance for bacteria *Klebsiella oxytoca* (see, for example, [10]). Most likely, that is why the magnetic properties of the ferrihydrite of these bacteria have not been adequately investigated. However, it is known from the extensive literature devoted to the ferritins of humans and animals [11–14] that these properties are well measurable and sufficiently pronounced that the ferritin (ferrihydrite) can be used in magnetic nanomedicine and bioengineering.

In this work, we examine the equilibrium magnetization curves for the biomineral ferrihydrite produced by the strain *Klebsiella oxytoca* separated from sapropel of Lake Borovoe (Krasnoyarsk Krai, Russia) [15–17]. Since these bacteria are easily reproduced under laboratory conditions, they can be used as "biofactories" for manufacturing these nanoparticles. As was shown in our earlier works [15–17], bacteria *Klebsiella oxytoca* during the growth produce the ferrihydrite of two types. The differences between these modifications are well identified, and their quantitative ratio varies with time in a nonmonotonic manner. This inference was made for the first time from analyzing the Mössbauer spectra [17]. Below, we will demonstrate that both types of nanoparticles synthesized by bacteria *Klebsiella oxytoca* can be identified using a more simple technique, i.e., static magnetic measurements.

2. MAGNETIC PROPERTIES OF ANTIFERROMAGNETIC NANOPARTICLES

The foundation of physics of nanodispersed antiferromagnets was laid almost fifty years ago by Néel [18, 19]. In [18], the conclusion was drawn that, in antiferromagnetic nanoparticles, the complete magnetic compensation of sublattices is impossible for a number of reasons, such as a small number of spins, the presence of cluster faceting, a defect lattice structure, etc. As a result, this particle should have an equilibrium magnetic moment μ and, at a finite temperature, should become superparamagnetic in the same sense that is used for small ferromagnetic particles.

Néel considered several variants for evaluating the magnetic moment μ. The simplest variant is random disturbances of the spin order. Then, the following relationship immediately follows from statistical considerations:

$$\mu \sim \mu_B z N^{1/2}, \quad (1)$$

where z is the number of uncompensated spins per atom, μ_B is the Bohr magneton, and N is the number of magnetic atoms. For a particle size of ~2–10 nm, the number of magnetic atoms is of the order of $N \sim 10^2$–10^5. Therefore, the magnetic moment of this object should amount to 1–10% of the corresponding value for a massive ferromagnet or ferrite with an equal volume. By using a characteristic magnetization of 400 G (maghemite or magnetite), we find that the effective spontaneous magnetization lies in the range from several gausses to several tens of gausses. It can be seen that this value is not small and considerably larger than, for example, the magnetization of weak ferromagnets. However, it should be remembered that hypothesis (1) is particularly model.

Under the assumption that the antiferromagnet consists of two simple sublattices, their magnetic moments in the particle are designated as $\mathbf{m}_1$ and $\mathbf{m}_2$. With allowance made for the decompensation, the magnitudes of the magnetic moments can be written in the form

$$m_1 = \mathcal{M}_s v + \frac{1}{2}\mu, \quad m_2 = \mathcal{M}_s v - \frac{1}{2}\mu, \quad (2)$$

so that we have $m_1 - m_2 = \mu$. Here, $\mathcal{M}_s$ is the magnetization of the sublattice in the massive sample and v is the particle volume. At temperatures significantly lower than the Néel point, the uncompensated magnetic moment is assumed to be constant in magnitude. This assumption is valid until the external field is substantially lower than the exchange field. Under these conditions, the antiferromagnetic vector is $\mathbf{e} = (\mathbf{m}_1 - \mathbf{m}_2)/2\mathcal{M}_s v$ and should retain its magnitude; in this case, the rotation of the vector is the only possible type of motion. In the nanodispersed antiferromagnetic particle, the vector $\mathbf{e}$ specifies the direction of the uncompensated magnetic moment

$$\mu = \mu \mathbf{e}.$$

It is known (see, for example, [20]) that the magnetic susceptibility of the antiferromagnet is anisotropic and its value along the normal to the antiferromagnetic vector is maximum. This mechanism of the reversible magnetization is associated with the "elastic canting" of the sublattices with respect to each other under the applied magnetic field. It should be noted that, according to another Néel hypothesis (the so-called superantiferromagnetism) [19], the magnetic susceptibility in small particles increases as compared to the massive crystal. As a consequence, the effective volume susceptibility of the nanoparticle can exceed this quantity of the macrocrystal by a factor of 2–3, which is confirmed by measurements [11, 12].

The induced magnetic moment is described by the linear susceptibility tensor

$$\chi_{ik} = \chi_A(\delta_{ik} - e_i e_k), \quad (3)$$

which is defined per unit volume of the particle. In the coordinate system where the Oz axis is aligned with the vector $\mathbf{e}$, the linear susceptibility tensor (3) has a diagonal form: the zz component of the tensor is equal to zero, and the other two components are positive and equal to each other. By expressing the magnetic moments of the sublattices from relationships (2) and (3), we obtain

$$\mathbf{m}_{1,2} = \left[\pm \mathcal{M}_s v + \frac{1}{2}\mu - \frac{1}{2}\chi_A v(\mathbf{eH})\right]\mathbf{e}, \quad (4)$$

where signs "plus" and "minus" are chosen for sublattices 1 and 2, respectively. Under these conditions, the energy of the particle takes the form

$$U = -\mu(\mathbf{eH}) + \frac{1}{2}\chi_A v(\mathbf{eH})^2, \quad (5)$$

where the coefficient of 1/2 in the second term, as usual, is due to the integration over the field.

The magnetic anisotropy is assumed to be uniaxial, and the energy density of the magnetic anisotropy and the unit vector of the easy magnetization direction are designated as K and $\mathbf{n}$. By adding the corresponding contribution to expression (5), we find the energy of the nanodispersed antiferromagnetic particle

$$U = -\mu(\mathbf{eH}) + \frac{1}{2}\chi_A v(\mathbf{eH})^2 - Kv(\mathbf{en})^2. \quad (6)$$

As can be seen from this formula, the magnetic state is completely determined by the orientation variables $\mathbf{e}$ and $\mathbf{n}$, i.e., the unit vectors of the magnetic moment and the anisotropy axis. In this respect, formula (6) is similar to the phenomenological relationship for the orientation-dependent part of the magnetic energy of a single-domain ferromagnetic particle. However, formula (6) contains not one but two field-dependent terms with minima corresponding to different points in the orientation space $\mathbf{e} \otimes \mathbf{n}$, which leads to the competition between the equilibrium orientation states of the particle. It can be seen from formula (6) that, if the particle can freely rotate (for example, if it is suspended in a fluid), the $\mathbf{n}$ axis of the particle becomes parallel to the vector $\mathbf{H}$ in the constant field $H < \mu/\chi_A v$ and the particle axis takes a canted position with respect to the vector $\mathbf{H}$ at $H > \mu/\chi_A v$. In this case, as the field increases, the canting smoothly increases and asymptotically tends to 90°. Therefore, at $H_* = \mu/\chi_A v$, the orientation of the suspension of nanodispersed antiferromagnetic particles exhibits a crossover: the system in the "easy-axis" state at $H < H_*$ transforms into a cone phase at $H > H_*$, which gradually approaches an "easy-plane" configuration. The same considerations determine the field H_* for the fixed particle, with the only difference that, in this situation, the position of the $\mathbf{n}$ axis is fixed and the equilibrium orientation of the magnetic moment varies.

Now, we determine the set of dimensionless parameters characterizing the nanodispersed antiferromagnetic particle. The ratio

$$\xi = \mu H/kT \quad (7)$$

(the Langevin argument) appears to be considerably smaller than that for ferroparticles of the same size due to the smallness of the uncompensated magnetic moment. However, the parameter

$$\sigma = Kv/kT \quad (8)$$

determining the probability of thermal-fluctuation magnetization reversal of the particle (supermagnetism) remains identical to that for ferroparticles with the same anisotropy. The third parameter represented in the form

$$\kappa = \frac{1}{2}\chi_A v H^2/kT \quad (9)$$

is characteristic only of antiferromagnets.

3. STATIC MAGNETIZATION

A gas of noninteracting magnetic dipoles is a convenient model for the analysis of magneto-orientational properties of the nanodispersed antiferromagnet. This approximation, which in physics of magnetic fluids is valid only for very dilute systems, in the case of the nanodispersed antiferromagnets (both colloidal and solid) has a fundamental justification. Since the dipole interaction is proportional to the square of the magnetic moment of the particle, this factor for the nanodispersed antiferromagnets turns out to be four to six orders of magnitude smaller than that for their ferromagnetic analogs. Therefore, the approximation of dilute systems holds true almost at any particle concentration [13].

The observed magnetic moment of the particle in a static ensemble is defined in a standard manner, i.e., as the derivative of the free energy with respect to the applied field: $\mathbf{m} = -\partial F/\partial \mathbf{H}$. From relationship (6), we obtain

$$m_i = \mu\langle e_i\rangle_0 + \chi_A v(\delta_{ik} - \langle e_i e_k\rangle_0)H_k, \quad (10)$$

where angular brackets with the subscript 0 indicate the averaging with the equilibrium distribution function $W_0 \propto \exp(-U/kT)$. In the general case, the magnetic moment $\mathbf{m}$ depends on the parameters given by formulas (7)–(9) and the angle between the easy-axis direction of the particle and the field.

The magnetization of the ensemble of noninteracting particles with the number concentration c is $\mathbf{M} = c\mathbf{m}$. For small ratios ξ, i.e., in weak fields, the magnetization can be determined analytically. In particular, for the solid dispersion with a random distribution of anisotropy axes, we find

$$M = \frac{1}{3}c\mu\xi\left[1 - \frac{1}{15}\xi^2(1+2S) - \frac{4}{15}\kappa(1-S)\right] + \frac{2}{3}c\mu q\left[1 - \frac{1}{15}(\xi^2 - 2\kappa)(1-S)\right]. \quad (11)$$

Here, it is convenient to use the temperature-independent dimensionless field strength $q = H/H_*$. In formula (11), we also introduced the equilibrium parameter of the orientation order $S = \langle P_2(\mathbf{en})\rangle_0$, where P_2 is the second-degree Legendre polynomial describing the orientation of the vector $\mathbf{e}$ with respect to the anisotropy axis of the particle. Therefore, the function S varies from zero (magnetically isotropic particle) to

unity (magnetically hard particle). Substitution $S = 0$ into expression (11) gives the classical result [18]

$$M = \frac{1}{3}c\mu\xi\left[1 - \frac{1}{15}(\xi^2 + 4\kappa)\right] + \frac{2}{3}c\mu q\left[1 - \frac{1}{15}(\xi^2 - 2\kappa)\right],$$

because Néel in his works ignored the particle anisotropy. For arbitrary fields, the magnetization for both solid and colloidal nanodispersed antiferromagnets is conveniently found from the system of equations relating the equilibrium means of the phase variables **e** and **n**. Problems of this type are effectively solved using the backward sweep method described, for example, in [21].

The magnetic anisotropy constant for nanodispersed antiferromagnets has a typical order of magnitude (for example, a few 10^5 erg/cm^3 for ferritin [12]). It can be seen from relationship (11) that, for a strong anisotropy ($\sigma \longrightarrow \infty$, $S_2 = 1$), the magnetic moment depends only on the parameter ξ for any Langevin arguments. Actually, for the strong anisotropy, the two-level approximation can be used instead of the complete calculation, which leads to the following expression for the magnetization:

$$M = c\mu[\tanh(\xi\cos\psi) + q(1 - \cos^2\psi)], \qquad (12)$$

where ψ is the angle between the easy-axis direction of the particle and the field. Recall that the parameter q is proportional to the field strength. For a random axis orientation, the integration of expression (12) leads to the formula [12]

$$M = c\mu\left[G(\xi) + \frac{2}{3}q\right], \quad G(\xi) = \int_0^1 \tanh(\xi y)dt. \qquad (13)$$

The last integral can be expressed through the known dilogarithm function

$$\mathrm{dilog}(x) = \int_1^x (1-t)^{-1}\ln t\,dt$$

(see, for example, [22]) in the form

$$G(\xi) = (1/24\xi^2)\{\pi^2 + 24\xi\ln[\exp(2\xi) + 1] - 12\xi^2 + 12\,\mathrm{dilog}[\exp(2\xi) + 1]\}.$$

Figure 1 compares the dependence $G(\xi)$ with the Langevin functions $L_1(\xi)$ and $L_2(\xi) = 1 - 3L_1/\xi$, which determine the magnetization in the ensembles formed either only by dipolar or only by polarizable (quadrupolar) particles, respectively. The asymptotic

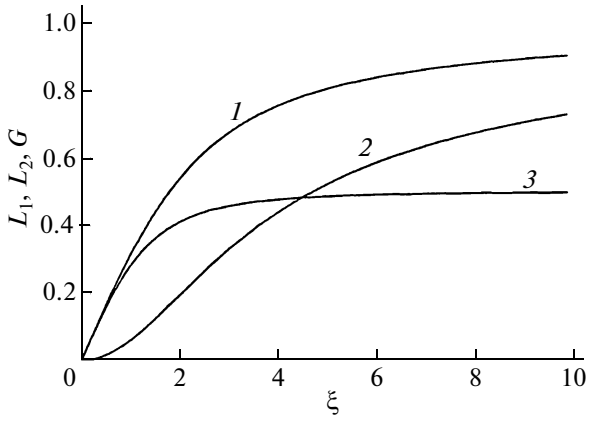

Fig. 1. Comparison of the Langevin functions (*1*) L_1 and (*2*) L_2 with (*3*) the function $G(\xi)$.

behavior of these functions is described by the relationships

$$G = \frac{1}{3}\xi - \frac{1}{15}\xi^3 + \ldots, \quad L_1 = \frac{1}{3}\xi - \frac{1}{45}\xi^3 + \ldots, \quad L_2 = \frac{2}{15}\xi^2 + \ldots \quad \text{at} \quad \xi \ll 1,$$
$$G = \frac{1}{2} - \frac{1}{24}(\pi^2/\xi^2) + \ldots, \quad L_1 = 1 - (1/\xi) + \ldots, \quad L_2 = 1 - (3/\xi) + \ldots \quad \text{at} \quad \xi \gg 1. \qquad (14)$$

It can be seen from these relationships that the function $G(\xi)$ coincides in the initial slope with the function $L_1(\xi)$ but reaches saturation considerably faster than the Langevin functions.

4. MEASUREMENT OF STATIC MAGNETIZATION CURVES

The microorganisms used were separated from the sapropel of Lake Borovoe (Krasnoyarsk Krai, Russia) by passing the taken samples through a magnetic separator. A bacterial biomass was grown under the microaerophilic and aerophilic conditions on a Lovley medium of the following composition: $NaHCO_3$, 2.5 g/l; $CaCl_2 \cdot H_2O$, 0.1 g/l; KCl, 0.1 g/l; NH_4Cl, 1.5 g/l; and $NaH_2PO_4 \cdot H_2O$, 0.6 g/l. The ferric citrate concentration was equal to 0.5 g/l, and the yeast extract concentration was 0.05 g/l. The bacteria were cultivated at different illuminances, including the complete dark. According to the Mössbauer spectroscopic investigations [17], the biomineral nanoparticles produced by bacteria *Klebsiella oxytoca* contain two magnetically ordered phases. Each phase is characterized by two states of Fe^{3+} ions with close values of the quadrupole splitting. In the phase conventionally termed Fe12, the quadrupole splitting is equal to 0.6–1.0 nm/s. In the phase called Fe34, the quadrupole splitting lies in the range 1.5–1.8 nm/s. According to

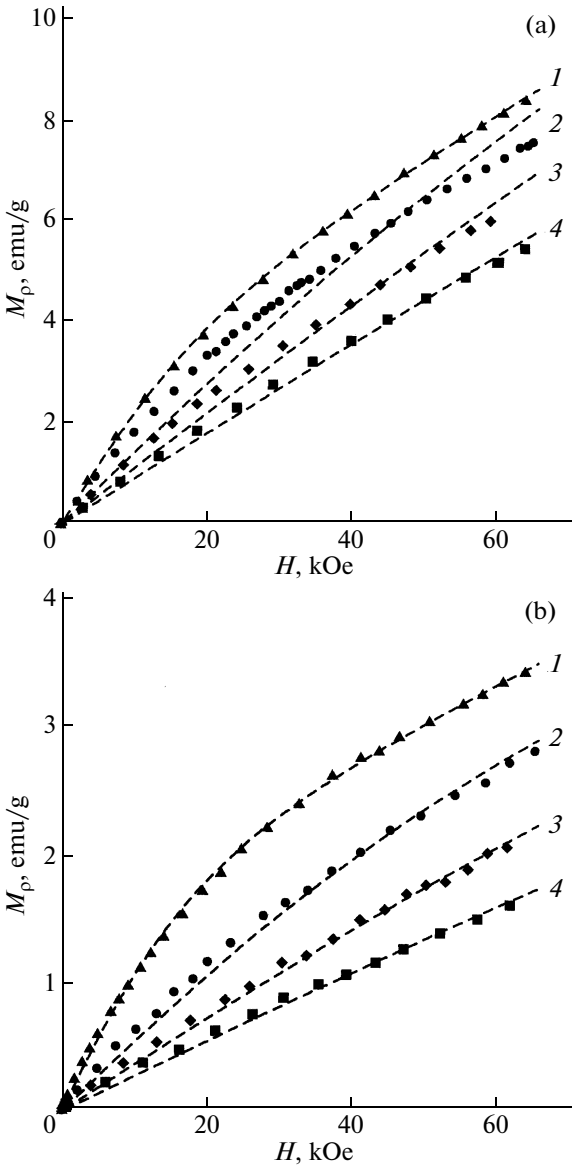

Fig. 2. Magnetizations of the (a) Fe12 and (b) Fe34 powders. Symbols indicate the experimental values at the temperatures $T = (1)$ 4.2, (2) 12, (3) 22, and (4) 33 K. Lines represent the results of the calculations from relationship (15) with the use of the magnetic parameters presented in the table.

the standard interpretation, the smaller values of the quadrupole splitting correspond to weaker local distortions in the lattice. By varying the conditions for the cultivation of microorganisms (duration, illumination, medium composition), the nanoparticles for which the states of Fe^{3+} ions were identified from the Mössbauer spectra either only as Fe12 or only as Fe34 were prepared for the magnetic measurements. The Fe12 and Fe34 powders studied in our work were separated from the biomass of microorganisms cultivated in the complete dark for 7 and 21 days, respectively.

The magnetization curves of the prepared ferrihydrite nanoparticles were measured on a vibrating-coil magnetometer with a superconducting solenoid [23] in the temperature range from 4.2 to 33 K in fields up to 65 kOe. At temperatures above ~40 K, the dependences $M(H)$ exhibit an almost linear behavior. In the field $H = 1$ kOe at high temperatures (150–300 K), the dependences of the quantity $1/M$ are linear in the temperature T. Their extrapolation to $1/M = 0$ gives the values of the asymptotic paramagnetic Curie temperature $\Theta_a \approx -600$°C and -100°C for the Fe34 and Fe12 powders, respectively.

5. EVALUATION OF THE PARAMETERS OF PARTICLES FROM THE MAGNETIZATION CURVE

It is assumed that the sample under investigation consists of identical ferrihydrite particles with random easy-axis orientations. In view of the low magnetization of the material, the difference between the internal and applied fields will be disregarded. For the same reason, the dipole–dipole interaction of particles should not noticeably affect the magnetization curve. Under these conditions, the function $M(H)$ is a superposition of partial curves (corresponding to individual particles). The averaging of the magnetization of particles in a powdered sample over random easy-axis directions of particles is performed using the above-derived formula (13), which for the case under consideration is conveniently represented in the form

$$M_\rho/\phi = \frac{2}{3}\chi_\rho H + I_\rho G(\alpha I_\rho H/T), \qquad (15)$$

where $M_\rho = M/\rho$ is the magnetization per unit mass of the sample and ϕ is the fraction of the magnetic phase in the sample. The right-hand side of relationship (15) contains the magnetic susceptibility $\chi_\rho = \chi_A/\rho$ and the magnetization $I_\rho = I_s/\rho$ per unit mass of the particle as the parameters. The quantity $\alpha = m_p/k$ is the ratio between the mass of the particle and the Boltzmann constant. As a result, the uncompensated magnetic moment is $\mu = m_p I_p$.

The theoretical magnetization curves for both samples (Fe12, Fe34) were calculated in the same way. Under the assumption that $\phi = 1$, the experimental points $M_\rho(H)$ at a temperature of 4.2 K were fitted by relationship (15). This procedure allowed us to obtain the numerical values of the quantities χ_ρ, I_ρ, and α. Then, by using the values obtained for the quantities I_ρ and α, the data on the magnetization $M_\rho(H)$ for the other three measurement temperatures were fitted by relationship (15) with the only fitting parameter χ_ρ. This made it possible to take into account the temperature dependence of the magnetic susceptibility, which was noted in a number of works concerned with the measurements of the animal ferritin [14]. The theoretical curves and the experimental magnetizations

Parameters χ_ρ (cm^3/g) in relationship (15) for the magnetization curves of the Fe12 and Fe34 samples

Sample	T, K			
	4.2	12	22	33
Fe12	1.28×10^{-4}	1.35×10^{-4}	1.23×10^{-4}	1.07×10^{-4}
Fe34	4.37×10^{-5}	3.66×10^{-5}	3.04×10^{-5}	2.49×10^{-5}

Note: $I_\rho = 6.25$ G cm^3/g and $\alpha = 4.64 \times 10^{-5}$ g deg/erg for the Fe12 sample and $I_\rho = 3.43$ G cm^3/g and $\alpha = 1.00 \times 10^{-4}$ g deg/erg for the Fe34 sample.

for the Fe12 and Fe34 powders are compared in Fig. 2. The corresponding numerical values of the parameters used in relationship (15) are listed in the table.

It can be seen from Fig. 2 that, on the whole, the aforementioned computational scheme allows us to satisfactorily fit the theoretical and experimental data. Now, the determined parameters of the curves $M(H)$ will be used to evaluate the average size of particles in the powders of the bacterial ferrihydrite. Initially, we consider the Fe12 sample. By using the value of α from the table, we find that the particle mass is $m_p = 6.3 \times 10^{-21}$ g. For a density $\rho \sim 4$ g/cm^3, this leads to a volume $v \sim 1.6 \times 10^{-21}$ cm^3. As a result, the average diameter is estimated to be $d \approx 1.5$ nm. This value is considerably smaller than that for the conventional ferritin, in which the particle size is as large as 7–8 nm. Indeed, for a ferrihydrite lattice constant of ~0.5 nm [24], the average diameter d is approximately equal to three spacings. Therefore, the inference can be made that the structural unit of the bacterial ferrihydrite is a crystallite in which magnetic atoms are predominantly located in the vicinity of the surface.

Now, we evaluate the magnetic properties of Fe12 particles. From the table for the same density, we have the magnetization $I_s = \rho I_\rho \sim 25$ G, which amounts to approximately 6% of the corresponding value for the massive sublattice. In this case, the magnetic moment of the particle is $\mu = m_p I_\rho \sim 4.0 \times 10^{-20}$ G cm$^3 \sim 4.3\mu_B$, which is of the order of the magnetic moment of one Fe^{3+} ion in the ideal spin-ordered lattice. However, in our case, the intrinsic (uncompensated) moment of the particle is a combined result of the incomplete orientation of several tens of spins. By assuming for the evaluation that $N \sim 50$, we find that the obtained value of I_s for the Fe12 sample appears to be approximately two times smaller than the value predicted by the hypothesis of random volume misorientation (1), according to which $\mu \propto N^{1/2}$. This is not surprising because expression (1) suggests that $N^{1/2}$ spins have an orientation antiparallel to the equilibrium orientation. In actual fact, this state would lead to an unjustified increase in the exchange energy. As follows from our data, the exponent in the relationship $\mu \propto N^\gamma$ is $\gamma \sim 0.3$.

Let us examine the properties of the Fe34 sample. According to the above procedure, we find $m_p = 1.36 \times 10^{-20}$ g and $v \sim 3.4 \times 10^{-21}$ cm^3. This leads to an average diameter $d \approx 1.8$ nm, which does not differ significantly from that for the Fe12 phase. For an estimated density $\rho \sim 4$ g/cm^3, the magnetization of the Fe34 sample is $I_s = \rho I_\rho \sim 14$ G, which amounts to approximately 3% of the corresponding value for the massive sublattice and is two times lower than that for the Fe12 sample. In this case, the magnetic moment of the particle is $\mu = m_p I_\rho \sim 4.2 \times 10^{-20}$ G cm$^3 \sim 4.5\mu_B$. By rounding the number of magnetic atoms to $N \sim 100$ for the evaluation, we find that, as for the Fe12 phase, the value of I_s for the Fe34 sample is considerably smaller than the value predicted by the hypothesis of random volume misorientation. As follows from our data, the exponent in the relationship $\mu \propto N^\gamma$ at $N \sim 100$ is $\gamma \sim 0.2$.

6. DISCUSSION OF THE RESULTS

The performed magnetic measurements confirm the presence of two fractions of biogenic ferrihydrite produced by bacteria *Klebsiella oxytoca*, which were previously revealed from analyzing the Mössbauer spectra. It follows from our data that the main difference lies in the magnetic susceptibility. It can be seen from the table that the parameter χ_ρ for the Fe12 particle is close to 10^{-4} cm^3/g, which is approximately three times larger than that for the Fe34 phase. In the Mössbauer spectra, the quadrupole splitting serves as the comparison parameter. According to the quadrupole splitting, the inference was made that the Fe12 crystallites are more ordered as compared to the Fe34 crystallites [17]. Most likely, this structural difference is responsible for the higher susceptibility of the Fe12 phase. Actually, the simultaneous fulfillment of two conditions is necessary for the appearance of the superantiferromagnetism (an increase in the magnetic susceptibility χ_ρ) [10]: the particle should be small (several lattice spacings in size) and have a pronounced crystal structure.

According to structural investigations, the X-ray diffraction patterns in the wavelength range 0.15–0.25 nm exhibit manifestations of two modifications of the mineral ferrihydrite, namely, the so-called two-line and six-line ferrihydrites [25], which are identified from the number of X-ray peaks. Both these modifications are crystalline phases, but the two-line phase has a considerably larger number of defects. In both

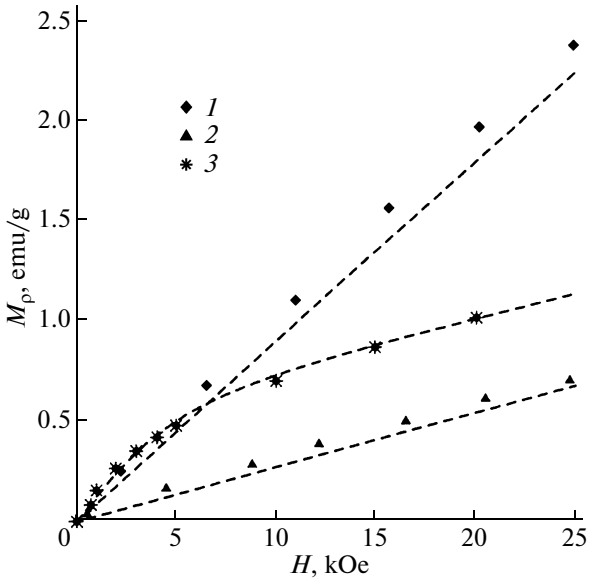

Fig. 3. Comparison of the magnetizations measured for the (*1*) Fe12 and (*2*) Fe34 powders at $T = 33$ K and (*3*) native ferritin at $T = 35$ K [26]. Dashed lines reproduce the curves shown for the ferrihydrite in Fig. 2 and the results of fitting for the ferritin [26].

phases of the mineral ferrihydrite, the characteristic size of X-ray coherent scattering regions amounts to ~2 nm [25], which quite correlates with the above estimates of the sizes of biogenic magnetic crystallites of both types. It should be noted that neither Mössbauer spectroscopy nor X-ray diffraction analysis have made it possible to elucidate whether these small particles are mechanically independent or they are joined together into large-sized dense aggregates. Electron microscopic examinations of this problem lead to contradictory results. The performed magnetic measurements only indicate that noticeable exchange or magnetic dipole interactions between these nanoobjects are absent.

Now, we compare the magnetization curves $M_\rho(H)$ for the samples under investigation with the corresponding dependences for their closest analog, i.e., the standard biogenic ferrihydrite (horse spleen ferritin). The corresponding data obtained in [26] at low temperatures for dry powders are compared with the results of our measurements in Fig. 3. The uncompensated magnetic moment of the horse spleen ferritin is evaluated to be $\mu = 345\mu_B$, which is approximately 70 times higher than that of the ferrihydrite produced by bacteria *Klebsiella oxytoca*. Therefore, the characteristic "Langevin" bend in the curve $M_\rho(H)$ for the horse spleen ferritin due to the response of the uncompensated moment is observed on the scale of Fig. 3 in lower fields and is significantly more pronounced than that for our particles. However, the specific parameters of horse spleen ferritin particles [26] are very similar to those of the ferrihydrite particles under investigation. Indeed, for the magnetic moment ratio equal to $345//4.5 \approx 77$, the cube of the ratio between the particle diameters is $(8/1.8)^3 \approx 87$, so that the effective magnetizations of both compounds are almost coincident: $I_s = \mu/v \sim 14$ G. This is the expected result, because the fraction of surface particles in both cases is large.

The data obtained by different authors on the magnetic susceptibility χ_ρ of the nanodispersed ferrihydrite and ferritin are characterized by a considerable spread. For example, the magnetic susceptibilities χ_ρ of the horse spleen ferritin and mineral ferrihydrite differ by one order of magnitude: from 10^{-5} to 10^{-4} cm^3/g [27]. It can be seen from Fig. 3 that the magnetic susceptibilities of the Fe34 particles and horse spleen ferritin particles [26] are very close to each other: the slopes of the curves in the high-filed range are almost identical. However, the magnetic susceptibility χ_ρ of the Fe12 particles is approximately three times higher. As was noted at the beginning of this section, it is this difference associated with the superantiferromagnetism that allows us to identify the Fe12 and Fe34 modifications in magnetic measurements as different phases.

Under the conditions of the superantiferromagnetism, the magnetic susceptibility of the ferrihydrite and ferritin particles becomes dependent on the temperature. A decrease in the magnetic susceptibility χ_ρ with the temperature was revealed in a number of experimental works [12, 24, 26, 27]. It should be noted that the case in point is the dependence $\chi_\rho(T)$ for the material of particles rather than the decrease in the observed magnetic susceptibility of the sample in proportion to $1/T$ due to the Langevin contribution to the magnetization $M_\rho(T)$. In our case, the dependences $\chi_\rho(T)$ for the Fe12 and Fe34 samples turn out to be different. Actually, the magnetic susceptibility χ_ρ of the Fe12 crystallites (hypothetically superantiferromagnetic) hardly decreases with the temperature, whereas the magnetic susceptibility χ_ρ of the less ordered Fe34 particles decreases substantially. The factors responsible for the revealed features of the dependences $\chi_\rho(T)$ call for further investigation.

7. CONCLUSIONS

Thus, it has been demonstrated that the magnetic measurements of nanoparticles consisting of the ferrihydrite produced by bacteria *Klebsiella oxytoca* make it possible to identify the presence of two different modifications of this compound, i.e., the Fe12 and Fe34 phases, in the samples. As a result, we have established that the structural differences revealed between crystallites of these modifications with the use of Mössbauer spectroscopy correlate well with the differences in their magnetic properties.

According to the magnetic grain-size estimates, the sizes of crystallites of both types are close to each other

(1.5–2.0 nm); however, the magnetic susceptibilities of the Fe12 and Fe34 particles differ substantially.

The established relationships between the magnetic and structural properties of the Fe12 and Fe34 phases significantly enhance the instrumental capabilities of investigating the bacterial ferrihydrite. Collected information on the magnetism of biomineral particles produced by bacteria *Klebsiella oxytoca* is useful for developing applications that suggest the use of natural antiferromagnetic nanodispersions as magnetically controlled functional materials.

ACKNOWLEDGMENTS

We would like to thank R.S. Iskhakov for helpful discussions.

This study was supported by the Russian Foundation for Basic Research (project nos. 07-02-96026, 07-02-96017, and 08-02-00802) and performed within the framework of the Federal Target Program "Research and Research–Pedagogical Personnel of Innovation Russia for 2009–2013."

REFERENCES

1. F. C. Meldrum, W. J. Wade, D. L. Nimmo, B. R. Heywood, and S. Mann, Nature (London) **349**, 686 (1991).
2. Z. Wang, C. Li, M. Ellenburg, E. Soistman, J. Ruble, B. Wright, J. X. Ho, and D. C. Carter, Acta Crystallogr., Sect. D: Biol. Crystallogr. **62**, 800 (2006).
3. P. D. Allen, T. G. St Pierre, W. Chua-anusorn, V. Ström, and K. V. Rao, Biochim. Biophys. Acta **1500**, 186 (2000).
4. Y. Gossuin, A. Roch, R. N. Müller, P. Gillis, and F. Lo Bue, Magn. Reson. Med. **48**, 959 (2002).
5. T. Z. Kidane, E. Sauble, and M. C. Linder, Am. J. Physiol. **291**, C445 (2006).
6. S.-L. Hsieh, Y.-C. Chiu, and C.-M. Kuo, Fish Shellfish Immunol. **21**, 279 (2006).
7. D. Resnick, K. Gilmore, Y. U. Idzerd, M. Klem, E. Smith, and T. Douglas, J. Appl. Phys. **95**, 7127 (2004).
8. A. Soriano-Portillo, M. Clemente-Leon, J. Gomez-Garcia, E. Coronado, N. Galvez, E. Colacio, and J. M. Dominguez-Vera, Synth. Met. **148**, 7 (2005).
9. V. V. Nikandrov, Usp. Biol. Khim. **40**, 357 (2000).
10. D. Schuler and R. B. Frankel, Appl. Microbiol. Biotechnol. **52**, 464 (1999).
11. S. F. Kylcone and R. Cywinski, J. Magn. Magn. Mater. **140–144**, 1466 (1995).
12. C. Gilles, P. Bonville, H. Rakoto, J. M. Broto, K. K. W. Wong, and S. Mann, J. Magn. Magn. Mater. **241**, 430 (2002).
13. F. Luis, E. del Barco, J. M. Hernández, E. Remiro, J. Bartolomé, and J. Tejada, Phys. Rev. B: Condens. Matter **59**, 11837 (1999).
14. C. Gilles, P. Bonville, K. K. W. Wong, and S. Mann, Eur. Phys. J. B **17**, 417 (2000).
15. S. V. Stolyar, O. A. Bayukov, Yu. L. Gurevich, E. A. Denisova, R. S. Iskhakov, V. P. Ladygina, A. P. Puzyr', P. P. Pustoshilov, L. A. Chekanova, and M. A. Bitekhtina, Materialovedenie, No. 7, 34 (2006).
16. S. V. Stolyar, O. A. Bayukov, Yu. L. Gurevich, E. A. Denisova, R. S. Iskhakov, V. P. Ladygina, A. P. Puzyr', P. P. Pustoshilov, and M. A. Bitekhtina, Neorg. Mater. **42** (7), 843 (2006) [Inorg. Mater. **42** (7), 763 (2006)].
17. S. V. Stolyar, O. A. Bayukov, Yu. L. Gurevich, V. P. Ladygina, R. S. Iskhakov, and P. P. Pustoshilov, Neorg. Mater. **43** (6), 725 (2007) [Inorg. Mater. **43** (6), 638 (2007)].
18. L. Néel, C. R. Hebd. Seances Acad. Sci. **252**, 4075 (1961); C. R. Hebd. Seances Acad. Sci. **253**, 9 (1961).
19. L. Néel, C. R. Hebd. Seances Acad. Sci. **253**, 203 (1961); C. R. Hebd. Seances Acad. Sci. **253**, 1286 (1961).
20. S. V. Vonsovskii, *Magnetism* (Nauka, Moscow, 1971; Wiley, London 1974), Chap. 23.
21. Yu. L. Raikher and V. I. Stepanov, Adv. Chem. Phys. **129**, 419 (2004).
22. *Handbook of Mathematical Functions with Formulas, Graphs, and Mathematical Tables*, Ed. by M. Abramowitz and I. A. Stegun (Dover, New York, 1964; Nauka, Moscow, 1979), Chap. 27.
23. A. D. Balaev, Yu. V. Boyarshinov, M. M. Karpenko, and B. P. Khrustalev, Prib. Tekh. Éksp., No. 3, 167 (1985); Available from VINITI, No. 69-85.
24. M. S. Seehra, V. S. Babu, A. Manivannan, and J. W. Lynn, Phys. Rev. B: Condens. Matter **61**, 3513 (2000).
25. J. L. Lambor and J. E. Dutrizac, Chem. Rev. **98**, 2549 (1998).
26. S. A. Makhlouf, F. T. Parker, and A. E. Berkowitz, Phys. Rev. B: Condens. Matter **55**, R 14717 (1997).
27. M. S. Seehra and A. Punnoose, Phys. Rev. B: Condens. Matter **64**, 132410-4 (2001).

Translated by O. Borovik-Romanova